The indoor model test of loess landslide instability induced by artificial rainfall in Tianshui area

Jing Meng[1]，Peng Xin[1*]，Chengjun Feng[1]，Peng Zhang[1]，Chengxuan Tan[1]，Tao Wang[1]

[1]Institute of Geomechanics, Chinese Academy of Geological Sciences, Beijing 100081, China

Abstract. The loess slope stability is influenced by rainfall and other factors. In order to find out the mechanism of loess slope instability, especially the influence of rainfall intensity and slope, the indoor model test was performed to study rainfall-induced loess landslide in Tianshui area, Gansu Province. Slope gradient and rainfall intensity are considered as variables, and their influence on slope stability are analyzed based on monitoring of soil suction and water content, and slope deformation process. The results show that the higher the rainfall intensity, the faster the infiltration rate. The volumetric moisture rate under heavy rainfall is more than 10% under small rainfall intensity. The steeper the slope, the lower the infiltration rate for the slope model. The loess slope is prone to overall sliding from bottom to top under the heavy rainfall, and easily lead to down-top retrogressive landslide under light rain.

1 Introduction

In recent years, many geological disasters occurred in China. And over 70% of the geological disasters are landslides which mainly occurred in the rainy season[1]. The direct economic loss caused by the landslide is as high as 20 billion yuan every year[2]. Especially in Tianshui area of Gansu Province, there are many landslides occurred every year during the rainy season. And the loess landslide which caused by rainfall is the mainly disaster in Tianshui area. With the implementation of the "One Belt One Road", the economy of Tianshui area develops quickly. However, these disasters restricted the development and construction. Therefore, studying the mechanism of rainfall landslide instability has great significance.

Rainfall landslides has been one of research focuses in geotechnical engineering field. The indoor rainfall simulation experiment is one of the preferred ways to study such problems at the present stage. On the indoor simulation test of slope, Wu Caiping[3] et al. took rainfall erosion on the slope surface of loess plateau as the prototype and designed an indoor experiment to study the influence of rainfall on the shape of barren loess slope. She found that the slope top infiltration rate is always higher than the slope surface. Through indoor rainfall model experiments, academician Cui Peng[4] et al. pointed that slope runoff and particulate matter transport were the main factors of shallow slope damage. Through the self-developed centrifugal rainfall equipment, Qian Jiyun[5] et al. made the centrifugal simulation experiment of soil slope under rainfall conditions, and concluded that the change rate of slope strain rate was consistent with that of moisture content. Through centrifuge experiment of rainfall-induced silty soil slope instability, Zhan Liangtong[6] et al. verified the effectiveness of the rainfall warning line, and pointed that the key to prevent slope instability is slope foot protection.

In order to further find out the influence of rainfall type on the stability of loess slope, we did this indoor rainfall model experiment, combined 3d laser scanners, analyzed the relationship between rainfall type and slope gradient and infiltration rate. Preliminary explained the instability mechanism of rainfall secondary loess slope.

2 Test model

2.1 General situation of test

The experimental sample was taken from a secondary loess slope in Tianshui area, Gansu Province. Measured the dry unit weight of the sample loess was 13.5 kN/m^3, saturated unit weight was 18.2 kN/m^3, internal friction angle was 36.5 °, the permeability coefficient was 1.52×10^{-5} m/s. The sample loess was sieved with a fine screen of 1.0mm. And then, adopted layered filling method, filled in 8 layers, each layers is 5cm thick, to ensure the integrity and uniformity of the model. The test site is located in the debris flow laboratory of Chengdu University of Technology.

2.2 Test apparatus

According to the rainfall type in Tianshui area, Gansu Province, we designed indoor artificial rainfall device, which was composed of model box, rainfall control

* Corresponding author: Peng Xin: xinpengcugs@126.com

system and monitoring system (Fig.1). The model box is 1.2m×0.4m×0.6m. The whole frame is welded by high strength angle steel. One side and top are open, while the other three sides are closed with tempered glass. And draw black square grid with side length of 5cm on the tempered glass. The rainfall control system[7-8] were composed of a water supply system, a hydraulic controller, a spray unit, and a metal frame. The raindrop generators has two types of sprinkler head by size[9], in order to simulate heavy rainfall and light rainfall. The big sprinkler head spray angle is about 75 °, and the small one is 65 °. The sprinkler head is fixed in the shape of a plum (Fig.2) and rainfall height is 3m. The rainfall intensity range is 20~180mm/h, rainfall uniformity is 91.0%. The diameter of raindrop in experimental is basically consistent with that of natural rainfall with the same intensity. The monitoring system includes hydrological monitoring and deformation monitoring. Hydrological monitoring instruments include matrix water potential sensor (MPS-6, Decagon, USA), soil water sensor (EC-5, Decagon, USA) and special data acquisition instrument (EM50). Deformation monitoring instrument adopts Optech ILRIS-3D laser scanner produced by Teledyne Optech.

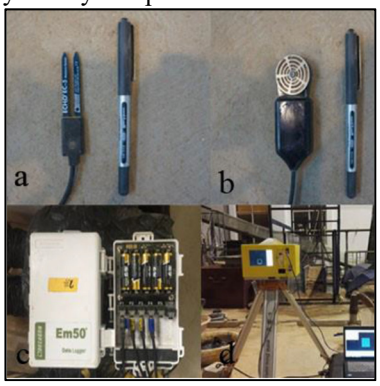

Fig.1. Test apparatus

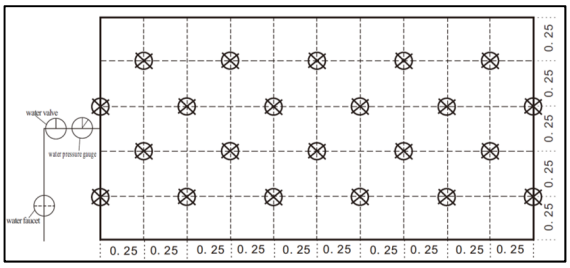

Fig.2. Sprinkler head diagram

3 Test method

According to relevant research[10-14], slope instability usually occurs in rain or after rain. Rainfall is an extremely important external cause of slope instability. Slope gradient is an important factor affecting slope stability. So, we set two variables-rainfall intensity and slope gradient in this experiment. The rainfall intensity are heavy rainfall of 115mm·h^{-1} and light rain of 45mm·h^{-1}. Slope gradient is set to 25°, 30°, 45°. Therefore, six indoor rainfall model experiments were designed. The detail working conditions see Table 1. The slope height is 40cm and the top platform is 20cm long. The location of water potential and water sensor is shown in Fig.3.

Table.1 Experiment working conditions

Test number	Initial pore water pressure /kPa	Initial water content /%	Rainfall intensity /(mm·h^{-1})	Gradient /(°)	Slope height /cm	remark
E-1	-413.67	6.92	115	45°	40	Barren loess slope
E-2	-415.95	6.82	115	30°	40	
E-3	-400.56	7.23	115	25°	40	
E-4	-385.90	6.80	45	45°	40	
E-5	-343.45	7.64	45	30°	40	
E-6	-420.68	6.84	45	25°	40	

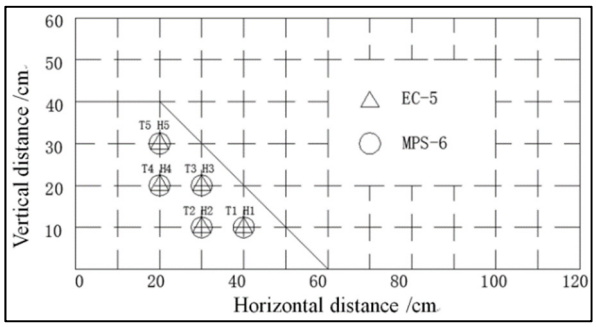

Fig.3. The location of water potential and water sensor

4 The slope instability process under different working conditions

According to different working conditions, this experiment was divided into six groups. Each group is buried 5 soil moisture sensors and 5 matrix suction sensors. The data acquisition frequency of EM50 is 2min/ time.

4.1 The slope instability process under continuous heavy rainfall

The first three groups of the experiment (E1 to E3) simulated the loess slope instability process under heavy rainfall. The instability mechanism of the slope was analyzed by hydrological monitoring and the change of slope shape. Taking E1 as an example, we analyzed the homogeneous slopes instability process under heavy rainfall.

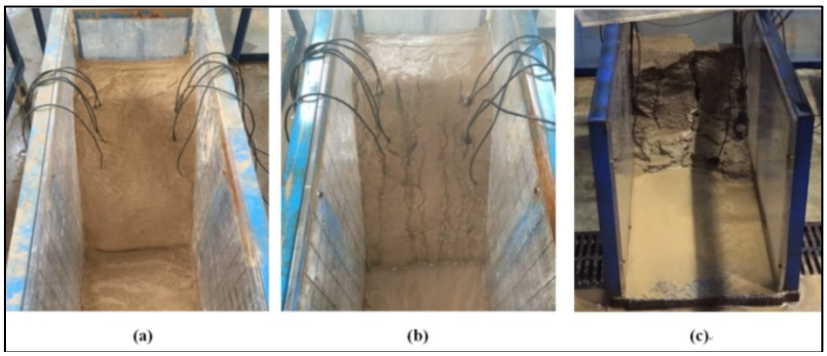

Fig.4. The homogeneous slopes instability process under heavy rainfall of E1

Fig.4 (a) shows the elevation of the initial state slope. The slope surface and top are flat. At the beginning of rainfall, the intensity of rainfall is less than the seepage velocity. The rainwater all seeped in the slope, with localized raindrop pits. Fig.4 (b) shows the runoff and local erosion began to appear on the slope, but the slope profile is still clear. As the rainfall continues, the slope appears obvious erosion streaks and slight loess collapsibility at the top of the slope. Fig.4 (c) is the final state after slope failure. Large scale collapse and sliding occurred in the front of the slope, resulting in high and steep free face at the back edge. The accumulation was carried far by the flowing water, and the top of the slope was obviously collapsibility.

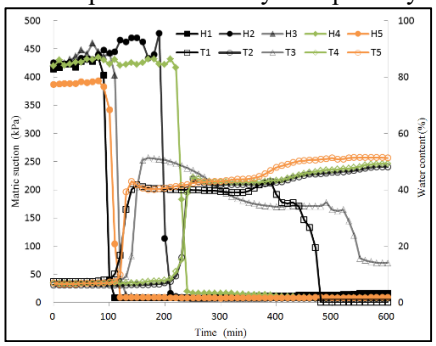

Fig.5. E1 curves of matric suction and water content vs. time under heavy rainfall

Fig.5 shows the change of water content with time under heavy rainfall. Under heavy rainfall, the response sequence of surface moisture sensor is T1-T3-T5. The infiltration velocity is slope foot faster than slope waist, slope waist faster than slope top. The water sensor T1 increases first, whose increasing rate goes from slow to fast to slow and then to stable. Take E1 as an example, there was no significant change in the sensor readings for a period of time after the rainfall began. But when the wetting front arrives, the sensor responds quickly. Soil water content increases and matrix suction decreases rapidly. Due to runoff erosion and local collapse of slope foot, T1 water sensor was exposed to air at 400min, while T3 was exposed at 500min. The water sensor's monitoring data began to fluctuate. Response time of T5, which was located at the top of slope, was later than T1 and T3 sensors.

4.2 The slope instability process under continuous light rain

E4 to E6 are light rain conditions. Taking E5 as an example, we analyzed the homogeneous slopes instability process under light rain.

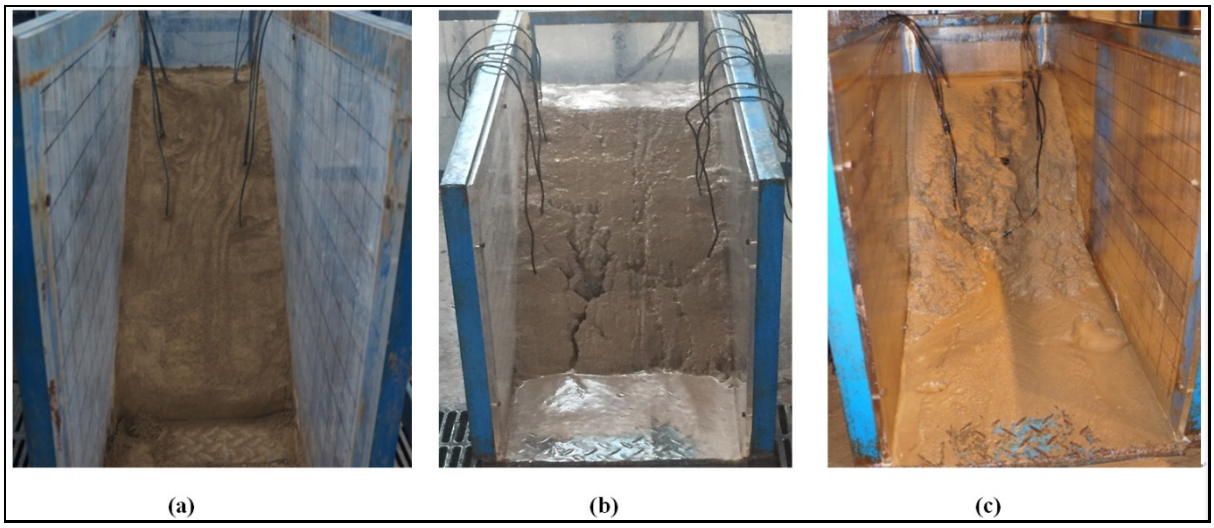

Fig.6. The homogeneous slopes instability process under light rain of E5

Fig.6 (a) shows the elevation of the initial state slope. The slope gradient is 30 °, and the slope outline is clearly. At the beginning of rainfall, the unpressurized seepage lasted about ten minutes, and no obvious phenomenon was left on the slope. Fig.6 (b) shows that runoff is formed on the slope surface, and a small landslide phenomenon caused by runoff erosion is formed on the slope foot. On the leading edge of the slope, there has generated a small amount of runoff transporting accumulation. But the slope profile is still clear. Fig.6 (c) shows the state of the slope after instability. Some sensors are exposed to air, and the leading edge of the slope has a large-scale collapse and slide. The profile from slope waist to top were relative integrity.

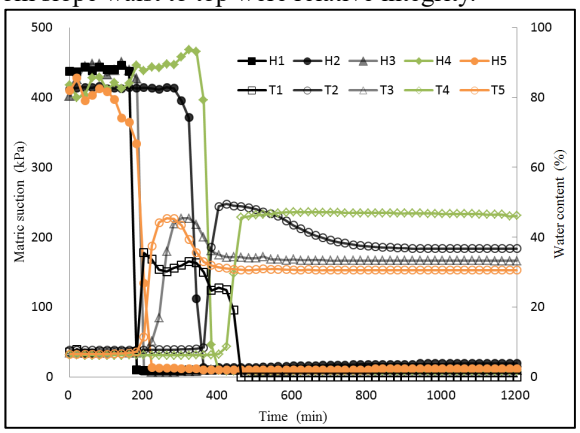

Fig.7. E5 curves of matric suction and water content vs. time under light rain

Fig.7 shows the change of water content with time under light rain. Under light rain, the response sequence of surface moisture sensor is T1-T5-T3. The infiltration velocity is slope foot faster than slope top, slope top fast than slope waist. The water sensor T1 increases first, T3 and T5 was slightly later than that at T1. Unlike continuous heavy rainfall, when the wetting front moves past the water sensor, the sensor becomes a transition zone, and its water content is slightly less than that at the wetting peak, then the water sensor display decreases slightly. Take E5 as an example, when the rainfall time reaches 240min, a small scale collapse of the slope foot caused T1 partial exposure, and the monitoring data happened slight fluctuations.

5 Effect of rainfall type on slope instability

Water seepage in soil is a complicated process. The current theoretical analysis and experimental methods are difficult to determine the true motion speed. So in practical engineering, we only consider the average velocity of macroscopic seepage flow. Under continuous uniform rainfall, the wetting front surface in the homogeneous loess slope is always parallel to the slope surface. We can calculate the rainwater infiltration rate during this period using the following formula.

$$v_{wetting\ front} = \frac{h \times \cos\alpha}{t} \quad (1)$$

$v_{wetting\ front}$ – The average movement speed of the wetting front over a period of time, m/s

h- The vertical height of the instrument, m

α- The slope gradient, (°)

t- The instrument response time, s

We used Formula (1) to calculate the movement speed of the wetting front. The calculation results are shown in Fig.8.

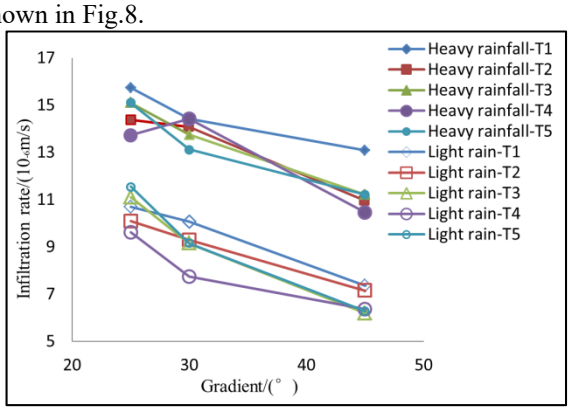

Fig.8. The infiltration rate changes with artificial rainfall

As shown in Fig.8, the infiltration rate decreases with the increase of gradient under heavy rainfall. In the gradient changes of 25 ° to 30 °, the infiltration rate decreased slightly. Slope from 30 ° to 45 °, the infiltration rate significantly reduced. The infiltration rate decreases with the increase of gradient in the light rain. When the gradient is constant, the infiltration rate under

heavy rainfall is always higher than that under light rain. The infiltration rate decreases with the increase of infiltration depth. Under the same 45 ° slope, heavy rainfall infiltration rate is faster than light rain 2 times. Slope to 30 °, the multiple decreases to 1.5 times. And when slope to 25 °, the multiple decreases to 1.3 times. With the decrease of the slope, infiltration rate has a tendency to decrease.

According to the analysis, the instability time of slope under heavy rainfall is always earlier than that under light rain. Under heavy rainfall, the water content of soil surface is about 40% when the slope sliding on a large scale. While under light rain, the water content is about 30%.

6 Conclusions

(1) Experimental results show that the slope infiltration rate is affected by rainfall type. Under heavy rainfall （115mm·h^{-1}）, the infiltration rate of slope top was the slowest. Under the condition of light rain（45mm·h^{-1}）, the infiltration rate of slope waist was the slowest. Within the scope of a certain gradient (25 °-45 °), the greater the gradient, the smaller the infiltration rate.

(2) The higher the rainfall intensity, the faster the infiltration rate of the model slope, and the slope is prone to instability. Under heavy rainfall, the slope is prone to integral sliding from bottom to top. And water content on the sliding surface is about 40%. Under light rain, it is easy to evolve into bottom-up retrogressive landslide, and the water content on the sliding surface is about 30%.

(3) Combined with the change chart of water content vs. time, it is suggested that, under heavy rainfall （115mm·h^{-1}）, the landslide early warning can be started if the rainfall time has maintained for 120min. Under light rain（45mm·h^{-1}）, the landslide early warning time should be 240min.

Acknowledgements

This work was supported by the projects: China Geological Survey (Grant No. DD20160267), and The Basic Science Foundation of Institute of Geomechanics (Grant No. 22).

References

1. National geological disaster notification, China geological environment information site, (2017)
2. International Federation of Red Cross and Red Crescent societies. World Disasters Report 1995 (R), (1996)
3. C. Wu, Y. Luo, W. Chen. Indoor Model Experiment for Rainfall Effects on Bare Loess Slope Shape. *Bulletin of Soil and Water Conservation*, **01**:121-125 (2013)
4. P. Cui, C. Guo, J. Zhou, et al. The mechanisms behind shallow failures in slopes comprised of landslide deposits. *Engineering Geology*, **S1**:34- 44 (2014)
5. J. Qian, G. Zhang, J. Zhang. Centrifuge model tests for deformation mechanism of soil slope during rainfall. *Rock and Soil Mechanics*, **02**:398-403 (2011)
6. L. Zhan, X. Liu, P. Qin. Centrifuge modelling of rainfall-induced slope failure in silty soils and validation of intensity-duration curves. *Chinese Journal of Geotechnical Engineering*, **36**:1784-1790 (2014)
7. D. Guo, X. Chen, J. Ma, et al. Reliability Analysis for Artificial Rainfall System Based on Raindrop Spectrum Detector. *Journal of Soil and Water Conservation*, **04**:88-93 (2015)
8. Y. Xu, Y. Liu, H Guo. Characteristics Research of Nozzle in the Artificial Rainfall System. *Mechanical Engineer*, **07**:16-18 (2013)
9. N. Xie, Z. Wang, W. Deng, et al. Field investigation and artificial rainfall simulation tests on unsaturated soil slopes. *Engineering Journal of Wuhan University*, **02**:81-85 (2008)
10. J. Wang, J. Li, Q. Li, et al. Analysis of influence factors of high slope stability of loess: Taking the Baojixia Water Division Project for example. *Rock and Soil Mechanics*, **30(7)**:2114-2118 (2009)
11. Y. Niu, J. Ma. A Study of the Effect Factor on Slope Stablility. *Research of Soil and Water Conservation*, **18 (04)**:278-281 (2011)
12. S. Zhang, S. Kang, Y. Li. Influence of Rainfall on Loess Slope Stability. *Bulletin of Soil and Water Conservation*, **05**:46-48 (2005)
13. C. Cheng, X. Chen, M. Tian. Influence of Rainfall Infiltration of Sandy Slope on Deformation and Stability. *Metal Mine*, **05**:180-185 (2015)
14. Y. Xia, L. Zhang. Numerical Analysis on Highway Slope Stability Considering Rainfall Infiltration. *Journal of Highway and Transportation Research and Development*, **10**:31-36 (2009)